Anomalous connection between antiferromagnetic and superconducting phases in the pressurized noncentrosymmetric heavy-fermion compound CeRhGe_{3}

Honghong Wang, Jing Guo, Eric D. Bauer, Vladimir A. Sidorov, Hengcan Zhao, Jiahao Zhang, Yazhou Zhou, Zhe Wang, Shu Cai, Ke Yang, Aiguo Li, Peijie Sun, Yi-feng Yang, Qi Wu, Tao Xiang, J. D. Thompson, and Liling Sun

Phys. Rev. B **99**, 024504 — Published 10 January 2019

DOI: 10.1103/PhysRevB.99.024504

Anomalous connection between antiferromagnetic and superconducting phases in pressurized non-centrosymmetric heavy fermion compound $CeRhGe_3$

Honghong Wang[1,5]*, Jing Guo[1]*, Eric D. Bauer[2], Vladimir A Sidorov[3], Hengcan Zhao[1,5], Jiahao Zhang[1,5], Yazhou Zhou[1,5], Zhe Wang[1,5], Shu Cai[1,5], Ke Yang[4], Aiguo Li[4], Peijie Sun[1], Yi-feng Yang[1,5], Qi Wu[1], Tao Xiang[1,5], J. D. Thompson[2]†, Liling Sun[1,5]†

[1]*Institute of Physics, Chinese Academy of Sciences, Beijing 100190, China*

[2]*Los Alamos National Laboratory, MS K764, Los Alamos, NM 87545, USA*

[3]*Institute for High Pressure Physics, Russian Academy of Sciences, 142190 Troitsk, Moscow, Russia*

[4]*Shanghai Synchrotron Radiation Facilities, Shanghai Institute of Applied Physics, Chinese Academy of Sciences, Shanghai 201204, China*

[5]*University of Chinese Academy of Sciences, Beijing 100190, China*

Unconventional superconductivity frequently emerges as the transition temperature of a magnetic phase, typically antiferromagnetic (AFM), is suppressed continuously toward zero temperature. Here, we report contrary behavior in pressurized $CeRhGe_3$, a non-centrosymmetric heavy-fermion compound. We find that its pressure-tuned AFM transition temperature (T_N) appears to avoid a continuous decrease to zero temperature by terminating abruptly above a dome of pressure-induced superconductivity. Near 21.5 GPa, evidence for T_N suddenly vanishes, the electrical resistance becomes linear in temperature and the superconducting transition reaches a maximum. Analysis of high-pressure resistance and X-ray absorption spectroscopy measurements suggest that the anomalous connection between antiferromagnetic and superconducting phases in pressurized $CeRhGe_3$ is associated with proximity to a critical valence instability.

PACS numbers: 74.70.Tx, 71.27.+a, 74.62.Fj

Experimental evidence suggests that magnetic fluctuations play an important role for the emergence of unconventional superconductivity, with that superconductivity often develops in the vicinity of a sufficiently suppressed antiferromagnetically (AFM) ordered state [1-6], as demonstrated in the copper-oxide [7,8], iron-based [9,10] and heavy-fermion superconductors [11,12]. A prominent common feature of their phase diagrams is that an AFM transition temperature (T_N) is suppressed continuously by pressure or chemical doping and presents a trend that it terminates at zero temperature, a magnetic quantum critical point, inside the superconducting phase. Over the past years, substantial efforts have been made to understand the interplay between AFM and superconducting phases, but it is still a challenging issue for condensed matter physics.

Heavy-fermion materials provide a particular opportunity to study this issue because they are highly tunable with pressure, which does not introduce chemical/site disorder. Among heavy-fermion compounds, the $CeTX_3$ (T = Co, Ir, Rh and X = Si, Ge) [13,14] family possess an interesting crystal structure without inversion symmetry. In their pressure-induced superconducting state, these non-centrosymmetric compounds are expected to show unconventional pairing and corresponding exotic physics [15-19]. Indeed, superconductivity in $CeIrSi_3$, $CeRhSi_3$, $CeCoGe_3$ and $CeIrGe_3$ [20-24] develops near an antiferromagnetic boundary and displays unusual properties, including a very large upper critical field [20-26] and strong magnetic anisotropy [25,26]. Thus, this family of non-centrosymmetric superconductors provides a special platform to explore and understand the connection between the magnetic and superconducting phases.

At ambient pressure, $CeRhGe_3$ is a heavy-electron antiferromagnet and, like other family members, crystallizes in the tetragonal $BaNiSn_3$-type structure, space group I4mm (no. 107) [13,19, 27]. Previously, we demonstrated that applied pressure induces superconductivity in $CeRhGe_3$ at a pressure above 19 GPa and argued that substantial Kondo and spin-orbit coupling favor superconductivity in it as well as in the broader $CeTX_3$ family [28]; however, the relationship between AFM and superconductivity in $CeRhGe_3$ is unusual. Unlike phase diagram's characteristic of pressure-induced superconductors in which the Néel temperature (T_N(P)) decreases continuously toward a zero-temperature magnetic/non-magnetic boundary inside a dome of superconductivity [6,11,12,17,18], the AFM transition temperature of $CeRhGe_3$ stays nearly constant over an extended pressure range before resistive evidence for order disappears abruptly at a pressure $P_C \sim 21.5$ GPa where the superconducting temperature T_C approaches its maximum value. This is illustrated in Fig. 1a where for clarity we show only the high-pressure part of the T-P phase diagram [28]. Sister compounds $CeIrGe_3$ [24] and $CeRhSi_3$ [21, 25] exhibit a similar relationship between AFM and superconductivity, and for comparison, T_N(P) for $CeIrGe_3$, which has a similar P_C, is included in this figure. The near temperature-linear electrical resistance of $CeRhGe_3$ in the vicinity of P_C is characteristic of a non-Fermi-liquid and is plotted in Figs. 1b and 1c. Though (quantum) critical magnetic fluctuations are known to produce a non-Fermi-liquid resistance [29] and are argued to favor formation of an unconventional superconducting state [30], there is no evidence from T_N(P) for the underlying origin

of these fluctuations, a magnetic quantum-critical point, in $CeRhGe_3$. Like critical magnetic fluctuations, critical valence fluctuations may induce a non-Fermi-liquid state and have been proposed as a mechanism for developing superconductivity in pressurized Ce- and Yb- based heavy-fermion compounds as decreasing cell volume increases the mean valence of Ce or Yb ions toward a critical instability of their *f*-shell occupancy [11, 31-33]. X-ray absorption measurements at energies around the L_{III}-edge of the 4*f* ion are a well-documented method for determining the mean 4*f* valence [34]; however, these measurements are challenging at very high pressures because the diamond anvil used for creating pressure absorbs X-rays by ~90% at the energy of Ce's L_{III}-edge [35]. This substantially weakens a detectable spectral signal from the sample, and, consequently, there is less direct experimental evidence for the effect of valence fluctuations on developing superconductivity in pressurized Ce-based heavy fermion compounds. Nevertheless, to explore the possible role of the valence instability on the anomalous connection between antiferromagnetic and superconducting phases in pressurized $CeRhGe_3$, we made great effort to overcome these difficulties. As will be discussed, these L_{III}-edge measurements, combined with an analysis of the resistivity, indicate that the superconductivity found in $CeRhGe_3$ is associated with proximity to a critical valence instability.

We begin with resistance measurements obtained on a single crystal of $CeRhGe_3$ in a diamond anvil cell with NaCl as the pressure medium [28]. To avoid the effects of magnetic order, we fit the residual resistance (R_0) and power (n) at various pressures, from just below to above P_C, to a power law form $R = R_0 + AT^n$, where A is a

coefficient. The pressure dependences of n and R_0 are shown in insets of Fig.1a. From these fits, n is a minimum at P_C, while R_0 continuously decreases over the pressure range. The non-Fermi liquid behavior, *i.e.*, $n \approx 1$, is shown more clearly in Fig. 2a where we plot the temperature dependence of the exponent n derived from a logarithmic derivative, $\partial \ln(R(\mathrm{T})-R_0)/\partial \ln T$. A similar linear-in-temperature resistance appears in $CeIrGe_3$ near its critical pressure [24]. As an alternative to a power-law description of the resistance, we also fit these data to a two-component model proposed initially and used subsequently in studies of the non-Fermi liquid resistivity of cuprates [36,37]. In this model, R is the sum of T-linear and T^2 contributions, $R = R_0 + A\mathrm{T} + B\mathrm{T}^2$. In the same temperature and pressure ranges, fits of the resistance to this form are indistinguishable from a power-law fit, and resulting fit parameters are given in Figs. 2b, 2c and 2d. As seen in these plots, the residual resistance and T-linear coefficient approach a maximum near P_C; whereas, the quadratic coefficient is a minimum. These are responses expected near a critical valence instability [32, 38-40]. In this scenario, enhanced valence fluctuations increase the T-linear coefficient of resistance as well as scattering from sample defects and mediate superconducting pairing [32,38].

In light of these implications, their possible applicability to account for observations in Fig.1a and the expected increase in hybridization between f and conduction electrons $\langle V_{fc} \rangle$ at high pressures, we performed room-temperature L_{III}-edge X-ray absorption spectroscopy measurements in a partial fluorescence yield mode at the Shanghai synchrotron radiation facility [41]. These diamond-anvil cell

experiments used diamonds selected to have low birefringence and silicon oil to produce a nearly hydrostatic pressure environment. Pressure in the cell was determined by a standard ruby-fluorescence technique. Results of this work are presented in Fig. 3a, in which the relative intensity of each curve is normalized to an edge jump of unity. An example of a fit to these data is shown in the inset of Fig. 3a where we used an error background (dashed line) and two Gaussian components, $4f^1$(green) and $4f^0$(blue). A possible $4f^2$ contribution expected at an incident photon energy of 5719 eV could not be detected definitively and was ignored in these fits. As evident in Fig. 3a, intensity of the main peak associated with the $4f^1$ configuration is suppressed when pressure is applied, while intensity of a small satellite peak, which is attributed to the presence of the $4f^0$ configuration in the initial state, increases. We estimate the pressure dependence of the mean valence (v) of Ce ions by using a widely accepted method, $v = 3 + I(4f^0)/\{I(4f^1)+ I(4f^0)\}$, where $I(4f^0)$ and $I(4f^1)$ represent the amplitudes of the spectral main peak and satellite peak, respectively. The resulting pressure dependence of v is shown in Fig. 3b where we see that v increases approximately linearly from 3.06 at 3.6 GPa to 3.13 at 30.1 GPa. An increase in v, *i.e.*, decrease in 4*f* occupancy, under compression is typical of Ce materials due to an increase in $\langle V_{fc} \rangle$ [42-45], and when all data are fit to a linear expression over the entire pressure range (solid line in Fig. 3b), there is no discontinuity for change of slope in v(P) at P_C (21.5 GPa).

Support for the valence-change interpretation comes from a scaling analysis of resistance proposed by Seyfarth *et al* to argue for the presence of a valence

quantum-critical endpoint in heavy-fermion $CeCu_2Si_2$ [33]. Following this methodology, we plot in Fig. 4a the pressure dependence of resistance isotherms R^*(P) from which impurity scattering (the residual resistance R_0) is subtracted from the measured resistance, *i.e.*, $R^*(P) = R(P) - R_0(P)$, for temperatures from 2 K to 10 K. This temperature range is sufficiently low to minimize contributions from phonons and crystal-field effects to R^*(P). At each temperature, R^* begins to drop significantly above P_C, which, as argued in the case of $CeCu_2Si_2$ [33], reflects an increased delocalization of the 4*f* electrons. To help isolate in these data the effect of delocalization from temperature-dependent scattering, we plot in Fig. 4b a normalized resistance R_{nor}, defined as $R_{nor} = \{(R^* - R^*(P_{VC}))/R^*(P_{VC})\}$, where P_{VC} is the pressure that corresponds to a 50% drop in $R^*(P)$ compared to its value at P_C. The steepness of resistance drop at the midpoint, $\chi = |dR_{nor}/dP|_{P_{VC}}$, is shown in Fig. 4c, where it is obvious that χ increases on cooling as would be expected upon approaching the critical end point of a broadened, weakly first-order valence transition at higher temperatures. The dotted curve in Fig. 4b is a fit of the data to the form $\chi \propto (T - T_{cr})^{-1}$ that gives T_{cr} = -20 K, which in this context corresponds to the temperature at which there is a critical end-point of a line of (weakly) first-order valence transitions. Introducing a generalized distance h/θ from the critical end point (where $h = (P - P_{VC})/P_{VC}$ and $\theta = (T - T_{cr})/T_{cr}$), we plot R_{nor} as a function of h/θ in Fig. 4d. As in $CeCu_2Si_2$ [33], h/θ collapses all our data below 10 K onto a single curve. These results, combined with L_{III}-edge data, are consistent with pressured $CeRhGe_3$ being in proximity to a critical valence instability.

The red squares in Fig. 4a correspond to the pressures P_{VC}(T) at which R* drops by 50%. A smooth extension of these points to zero-temperature (red line) gives the pressure P_{cr} ~ 23 GPa. Though this extrapolation is somewhat arbitrary, any reasonable extrapolation would give P_{cr} within ~1.5 GPa of the critical pressure P_C where T_C reaches a maximum and evidence for magnetic order disappears, strongly suggesting a connection between them and that the non-Fermi-liquid resistance above T_C has its origin in critical valence fluctuations.

An increase in mean valence with compression (Fig. 3b) implies increased *f*-*c* hybridization that should lead to a monotonic decrease in T_M(P) toward a magnetic quantum-critical point. This, however, does not appear to be the case with $CeRhGe_3$. We have no definitive explanation for why T_M(P) becomes weakly pressure dependent below P_C, but inspection of the *T*-*P* phase diagram (Fig. 1a) shows that the Néel boundary begins to deviate from its trajectory toward T=0 already at a pressure well below P_C (or P_{cr}). In this pressure range, ~ 17 GPa, the mean valence has increased to about 3.09 from roughly 3.05 at atmospheric pressure. With such an increase, it is plausible that the nature of magnetic order has changed in such a way to become less dependent on the (indirect) magnetic exchange that mediates order. Because $CeRhGe_3$ and $CeIrGe_3$ have very similar phase diagrams and associated non-Fermi-liquid behaviors, it is reasonable that the underlying physics is the same in both. Clearly, these phase diagrams call for experiments and theory that would shed light on microscopic interactions at pressures above 17 GPa.

In summary, we have investigated the unusual relationship between

antiferromagnetic and superconducting states in pressurized $CeRhGe_3$ through high-pressure resistance and L_{III}-edge absorption measurements, as well as a corresponding analysis of the low-temperature resistance. These results are consistent with a pressure-induced valence instability playing an import role for the appearance of superconductivity, the abrupt disappearance of evidence for magnetic order, and a non-Fermi-liquid resistivity in the absence of a magnetic quantum-critical point. An increase in the mean valence of Ce ions to about 3.10 in $CeRhGe_3$ seems to be a threshold for these phenomena to develop. From an analysis of resistance data, we deduce that a critical end point is located at -20 K (T_{cr}) and that a line of broadened, (weakly) first-order valence transitions reaches T=0 at ~ 23 GPa (P_{cr}), a pressure close to the critical pressure P_C (21.5 GPa) where T_C is a maximum and the resistance exhibits a *T*-linear behavior. These results not only underscore the effects of valence fluctuation on superconductivity in pressurized Ce-based heavy-fermion compounds, but they also provide an experimental case to test or develop theoretical models. Indeed, the varied relationships among magnetism, criticality and superconductivity that are found in $CeTX_3$ are anticipated theoretically in this model of critical valence fluctuations and their interplay with magnetic order in heavy-fermion metals.

Acknowledgements

We thank Prof. Frank Steglich for fruitful discussions. Work in China was supported by the National Key Research and Development Program of China (Grant No. 2017YFA0302900, 2017YFA0303103, 2016YFA0300300 and 2015CB921303),

the NSF of China (Grants No. 11427805, No. 11404384, No. U1532267, No. 11604376, No. 11522435, No. 11774401), the Strategic Priority Research Program (B) of the Chinese Academy of Sciences (Grant No. XDB07020300). Work at Los Alamos National Laboratory was performed under the auspices of the U.S. DOE, Office of Basic Energy Sciences, Division of Materials Sciences and Engineering.

† Correspondence and requests for materials should be addressed to L.S. (llsun@iphy.ac.cn) and J.T (jdt@lanl.gov).

* These authors contributed equally to this work.

Reference:

[1] T. Shibauchi, A. Carrington, and Y. Matsuda, Annu. Rev. Condens. Matter Phys. **5**, 113 (2014).

[2] I. I. Mazin and M. D. Johannes, Nat. Phys. **5**, 141 (2009).

[3] J. Paglione and R. L. Greene, Nat. Phys. **6**, 645 (2010).

[4] E. Dagotto, Rev. Mod. Phys. **66**, 763 (1994).

[5] P. C. Dai, J. P. Hu, and E. Dagotto, Nat. Phys. **8**, 709 (2012).

[6] N. D. Mathur, F. M. Grosche, S. R. Julian, I. R. Walker, D. M. Freye, R. K. W. Haselwimmer, and G. G. Lonzarich, Nature (London) **394**, 39 (1998).

[7] H. Saadaoui, Z. Salman, H. Luetkens, T. Prokscha, A. Suter, W. A. MacFarlane, Y. Jiang, K. Jin, R. L. Greene, E. Morenzoni, and R. F. Kiefl, Nat. Commun. **6**, 6041 (2015).

[8] M. Fujita, T. Kubo, S. Kuroshima, T. Uefuji, K. Kawashima, K. Yamada, I. Watanabe, and K. Nagamine, Phys. Rev. B **67**, 014514 (2003).

[9] A. J. Drew, C. Niedermayer, P. J. Baker, F. L. Pratt, S. J. Blundell, T. Lancaster, R. H. Liu, G. Wu, X. H. Chen, I. Watanabe, V. K. Malik, A. Dubroka, M. Rössle, K. W. Kim, C. Baines, and C. Bernhard, Nat. Mater. **8**, 310 (2009).

[10] P. Cai, X. D. Zhou, W. Ruan, A. F. Wang, X. H. Chen, D.-H. Lee, and Y. Y. Wang, Nat. Commun. **4**, 1596 (2013).

[11] H. Q. Yuan, F. M. Grosche, M. Deppe, C. Geibel, G. Sparn, and F. Steglich, Science **302**, 2104 (2003).

[12] T. Park, V. A. Sidorov, F. Ronning, J.-X. Zhu, Y. Tokiwa, H. Lee, E. D. Bauer, R. Movshovich, J. L. Sarrao, and J. D. Thompson, Nature (London) **456**, 366 (2008).

[13] Y. Muro, D. Eom, N. Takeda, and M. Ishikawa, J. Phys. Soc. Jpn. **67**, 3601 (1998).

[14] P. Haen, P. Lejay, B. Chevalier, B. Lloret, J. Etourneau, and M. Sera, Journal of the Less Common Metals **110**, 321 (1985).

[15] L. P. Gor'kov and E. I. Rashba, Phys. Rev. Lett. **87**, 037004 (2001).

[16] F. Kneidinger, E. Bauer, I. Zeiringer, P. Rogl, C. Blaas-Schenner, D. Reith, and R. Podloucky, Physica C: Superconductivity and its Applications **514**, 388 (2015).

[17] B. D. White, J. D. Thompson, and M. B. Maple, Physica C: Superconductivity and its Applications **514**, 246 (2015).

[18] C. Pfleiderer, Rev. Mod. Phys. **81**, 1551 (2009).

[19] T. Kawai, H. Muranaka, M.-A. Measson, T. Shimoda, Y. Doi, T. D. Matsuda, Y. Haga, G. Knebel, G. Lapertot, D. Aoki, J. Flouquet, T. Takeuchi, R. Settai, and Y. Ōnuki, J. Phys. Soc. Jpn. **77**, 064716 (2008).

[20] I. Sugitani, Y. Okuda, H. Shishido, T. Yamada, A. Thamizhavel, E. Yamamoto, T. D. Matsuda, Y. Haga, T. Takeuchi, R. Settai, and Y. Ōnuki, J. Phys. Soc. Jpn. **75**, 043703 (2006).

[21] N. Kimura, K. Ito, K. Saitoh, Y. Umeda, H. Aoki, and T. Terashima, Phys. Rev. Lett. **95**, 247004 (2005).

[22] R. Settai, Y. Okuda, I. Sugitani, Y. Ōnuki, T. D. Matsuda, Y. Haga, and H. Harima, Int. J. Mod. Phys. B **21**, 3238 (2007).

[23] G. Knebel, D. Aoki, G. Lapertot, B. Salce, J. Flouquet, T. Kawai, H. Muranaka, R. Settai, and Y. Ōnuki, J. Phys. Soc. Jpn. **78**, 074714 (2009).

[24] F. Honda, I. Bonalde, K. Shimizu, S. Yoshiuchi, Y. Hirose, T. Nakamura, R. Settai, and Y. Ōnuki, Phys. Rev. B **81**, 140507(R) (2010).

[25] N. Kimura, K. Ito, H. Aoki, S. Uji, and T. Terashima, Phys. Rev. Lett. **98**, 197001 (2007).

[26] R. Settai, Y. Miyauchi, T. Takeuchi, F. Lévy, I. Sheikin, and Y. Ōnuki, J. Phys. Soc. Jpn. **77**, 073705 (2008).

[27] A. D. Hillier, D. T. Adroja, Manuel, V. K. Anand, J. W. Taylor, K. A. McEwen, B. D. Rainford, and M. M. Koza, Phys. Rev. B **85**, 134405 (2012)

[28] H. H. Wang, J. Guo, E. D. Bauer, V. A. Sidorov, H. C. Zhao, J. H. Zhang, Y. Z.

Zhou, Z. Wang, S. Cai, K. Yang, A. G. Li, X. D. Li, Y. C. Li, P. J. Sun, Y.-F. Yang, Q. Wu, T. Xiang, J. D. Thompson, and L. L. Sun, Phys. Rev. B **97**, 064514 (2018).

[29] H. v. Löhneysen, A. Rosch, M. Vojta, P. Wölfle, Rev. Mod. Phys. 79, 1016 (2007).

[30] P. Monthoux, D. Pines, G. G. Lonzarich, Nature 450, 1177(2007).

[31] J. L. Sarrao, C. D. Immer, Z. Fisk, C. H. Booth, E. Figueroa, J. M. Lawrence, R. Modler, A. L. Cornelius, M. F. Hundley, G. H. Kwei, J. D. Thompson, and F. Bridges, Phys. Rev. B **59**, 6855 (1999).

[32] S. Watanabe and K. Miyake, Journal of Physics: Condensed Matter **23**, 094217 (2011).

[33] G. Seyfarth, A. S. Rüetschi, K. Sengupta, A. Georges, D. Jaccard, S. Watanabe, and K. Miyake, Phys. Rev. B **85**, 205105 (2012).

[34] R. D. Parks, S. Raaen, M. L. denBoer, V. Murgai, T. Mihalisin, Phys. Rev. B 28, 3556 (1983).

[35] R. Ingalls et al, Journal of Applied Physics 56(6), 3158(1980).

[36] A. P. Mackenzie, S. R. Julian, D. C. Sinclair and C. T. Lin, Phys. Rev. B 53, 5848 (1996).

[37] R. A. Cooper, Y. Wang, B. Vignolle, O. J. Lipscombe, S. M. Hayden, Y. Tanabe, T. Adachi, Y. Koike, M. Nohara, H. Takagi, C. Proust, and N. E. Hussey, Science **323**, 603 (2009).

[38] Y. Onishi and K. Miyake, J. Phys. Soc. Jpn. **69**, 3955 (2000).

[39] A. T. Holmes, D. Jaccard, and K. Miyake, Phys. Rev. B **69**, 024508 (2004).

[40] A. T. Holmes, D. Jaccard, and K. Miyake, J. Phys. Soc. Jpn. **76**, 051002 (2007).

[41] Y. Z. Zhou, D.-J. Kim, P. F. S. Rosa, Q. Wu, J. Guo, S. Zhang, Z. Wang, D. F. Kang, W. Yi, Y. C. Li, X. D. Li, J. Liu, P. Q. Duan, M. Zi, X. J. Wei, Z. Jiang, Y. Y. Huang, Y.-F. Yang, Zachary Fisk, L. L. Sun, and Z. X. Zhao, Phys. Rev. B **92**, 241118(R) (2015).

[42] H. Yamaoka, Y. Yamamoto, E. F. Schwier, F. Honda, Y. Zekko, Y. Ohta, J. F. Lin, M. Nakatake, H. Iwasawa, M. Arita, K. Shimada, N. Hiraoka, H. Ishii, K. D. Tsuei, and J. Mizuki, Phys. Rev. B **92**, 235110 (2015).

[43] H. Yamaoka, I. Jarrige, N. Tsujii, A. Kotani, J.-F. Lin, F. Honda, R. Settai, Y. Ōnuki, N. Hiraoka, H. Ishii, and K.-D. Tsuei, J. Phys. Soc. Jpn. **80**, 124701 (2011).

[44] H. Yamaoka, Y. Ikeda, I. Jarrige, N. Tsujii, Y. Zekko, Y. Yamamoto, J. Mizuki, J. F. Lin, N. Hiraoka, H. Ishii, K. D. Tsuei, T. C. Kobayashi, F. Honda, and Y. Ōnuki, Phys. Rev. Lett. **113**, 086403 (2014).

[45] J. P. Rueff, S. Raymond, M. Taguchi, M. Sikora, J. P. Itié, F. Baudelet, D. Braithwaite, G. Knebel, and D. Jaccard, Phys. Rev. Lett. **106**, 186405 (2011).

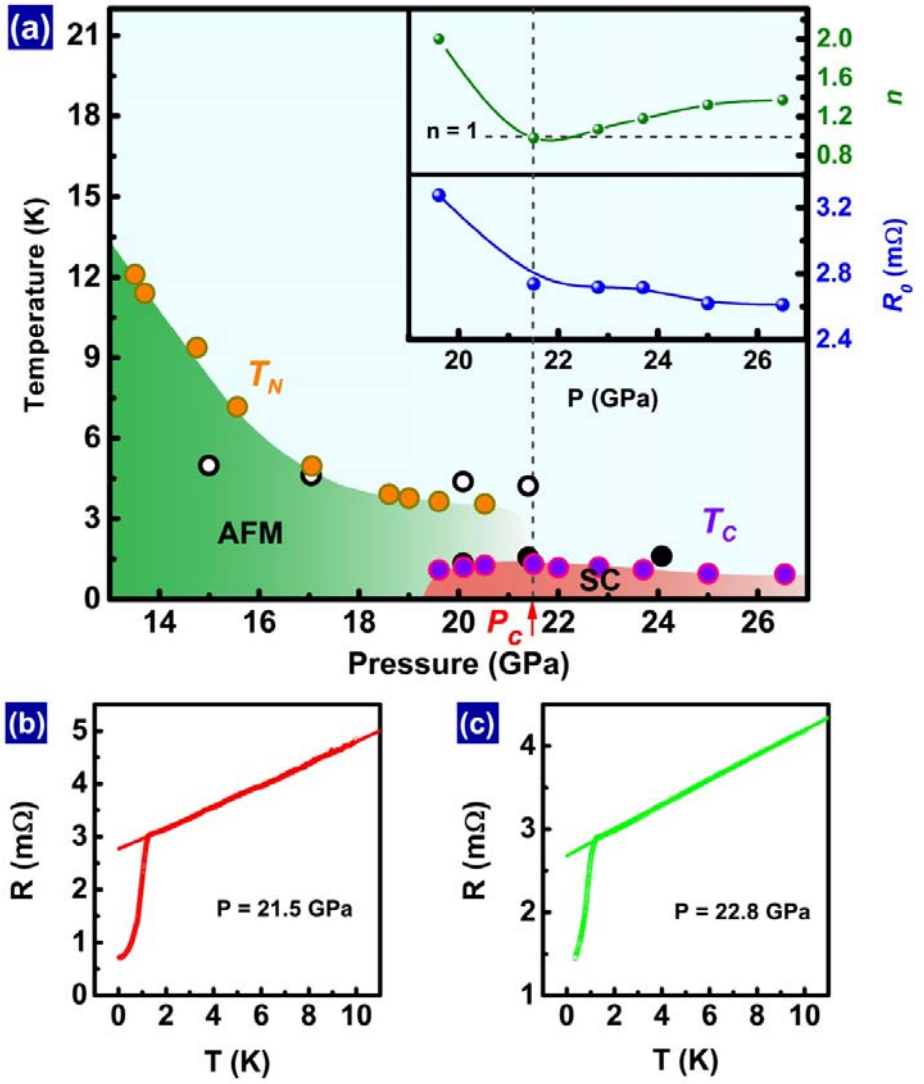

Figure 1 Temperature-pressure phase diagram and resistance versus temperature for $CeRhGe_3$. (a) Evolution of the AFM transition temperatures T_N and superconducting transition temperatures T_C with pressure for $CeRhGe_3$ and $CeIrGe_3$. The orange and purple solids represent the T_N and T_C of $CeRhGe_3$, respectively. These data are determined from resistance and *ac* susceptibility measurements [28]. The open and filled black circles stand for the T_N and T_C of $CeIrGe_3$, which are taken from Ref. [24]. Insets show the pressure dependence of parameters obtained from a fit of four-probe resistance measurements on $CeRhGe_3$ to the power-law form $R = R_0 + AT^n$,

as discussed in the text. P_C represents a critical pressure where magnetic order disappears abruptly and T_C displays a maximum. (b) and (c) Four-probe resistance as a function of temperature at 21.5 GPa and 22.8 GPa, showing T-linear behavior over an order of magnitude change in temperature above T_C. For reference, the absolute resistivity at atmospheric pressure and room temperature is 105 μΩcm and the resistance ratio ρ(300K)/ρ(2K) of this crystal is about 13.

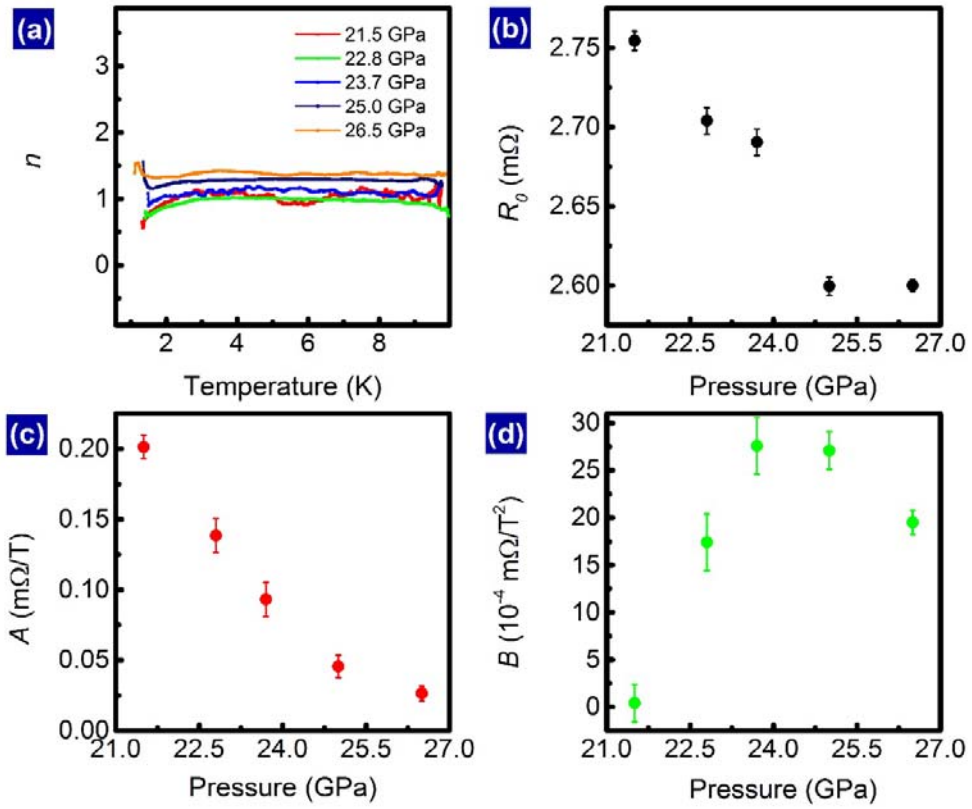

Figure 2 Parameters characterizing the low temperature resistance of $CeRhGe_3$ at $P \geq P_C$. (a) Exponent n of a power-law temperature variation of the resistance determined from a logarithmic derivative $\partial \ln(R(T)-R_0)/\partial \ln T$, assuming $R(T) = R_0 + AT^n$. (b)-(d) Parameters obtained from fitting the resistance to $R(T) = R_0 + AT + BT^2$. See text for details.

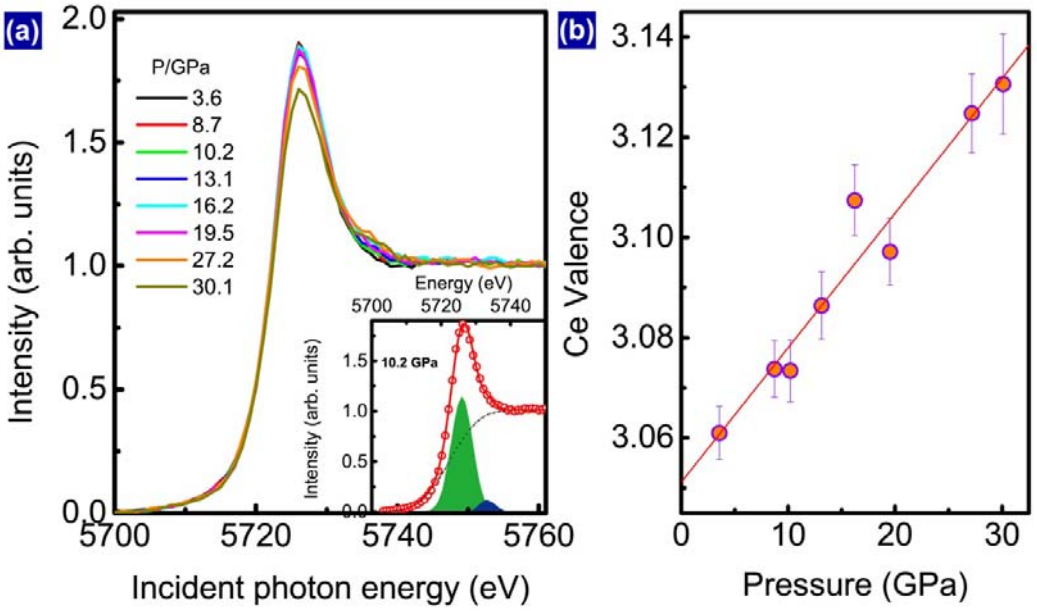

Figure 3 Results of high-pressure X-ray absorption measurements. (a) Ce-L_{III} X-ray absorption spectra of $CeRhGe_3$ at various pressures and room temperature. Inset shows an example of fits to the measured data (red open circles) and the result of curve-fitting (red solid curve). The green and blue areas are the results of Gaussian fits to $4f^1$ and $4f^0$ components. Background is represented by the black dashed curve. (b) Pressure dependence of the mean valence of Ce ions in $CeRhGe_3$. The solid line is a linear fit to all data.

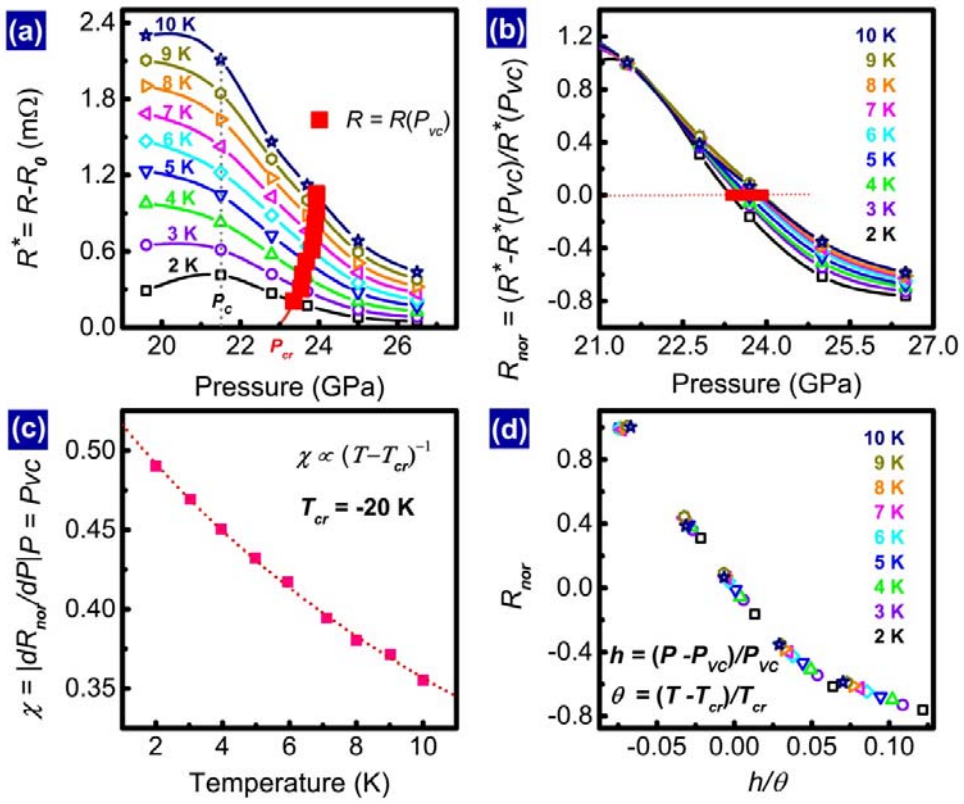

Figure 4 Scaling analysis of low-temperature resistance for $CeRhGe_3$ at pressures near $P_C \approx 21.5$ GPa. (a) Pressure dependence of the isothermal resistance R^* ($R^* = R - R_0$) at selected temperatures. Resistance data are adopted from Ref. [28]. The red squares indicate the pressure P_{VC} and the temperature at which R^* drops by 50% from its value at $P_C \sim 21.5$ GPa, and the red line is an extrapolation of the square data to P_{cr}. (b) Normalized resistance R_{nor} ($R_{nor} = [R^* - R^*(P_{VC})]/R^*(P_{VC})$) as a function of pressure. The red squares are equivalent to those presented in figure (a). (c) Temperature dependence of the slope χ ($\chi = |dR_{nor}/dP|_{P_{VC}}$). The red dashed line represents a Curie-Weiss fit, yielding $T_{cr} = -20$ K. (d) Collapse of normalized R_{nor} data as a function of generalized distance h/θ from the critical end point, where $h = (P - P_{VC})/P_{VC}$ and $\theta = (T - T_{cr})/T_{cr}$.